

Well-Log Derived Geomechanical Analysis of Microseismicity in the Mt. Simon Saline Aquifers (Illinois Basin - Decatur Project)



Eugene Myshakin^{1,2}; Abhash Kumar^{1,2}; William Harbert^{1,3}; Erich Zorn¹; Guoxiang Liu¹; Hema Siriwardane¹

¹National Energy Technology Laboratory, 626 Cochran Mill Road, Pittsburgh, PA 15236, USA; ²NETL Support Contractor, 626 Cochran Mill Road, Pittsburgh, PA 15236, USA; ³University of Pittsburgh, 4200 5th Avenue, Pittsburgh, PA 15260, USA

Science-informed Machine Learning to Accelerate Real Time (SMART) Decisions in Subsurface Applications

INTRODUCTION

The Illinois Basin - Decatur Project (IBDP) successfully demonstrated the safe geologic storage of carbon dioxide at a commercial scale. Within the IBDP project three deep wells (injection (CCS1), monitoring (VW1), geophysical (GM1)) were completed and geophysical logs were recorded. During injection and post-injection periods, microseismic monitoring was conducted to create a microseismic catalog. The correlations between microseismic attributes and geomechanical well logs define major geomechanical drivers of microseismic expression to understand a reservoir response to CO₂ injection in geological context. Utilizing standard sonic and density well logs, the dynamic elastic moduli were calculated and employed to correlate with microseismic pseudo-logs. Multi-dimensional Mu-rho and Lambda-rho (MRLR) hyperdimensional plots display meaningful data and uncovered subtle relationships between elastic properties of sandstones and the seismological attributes of recorded microseismicity.

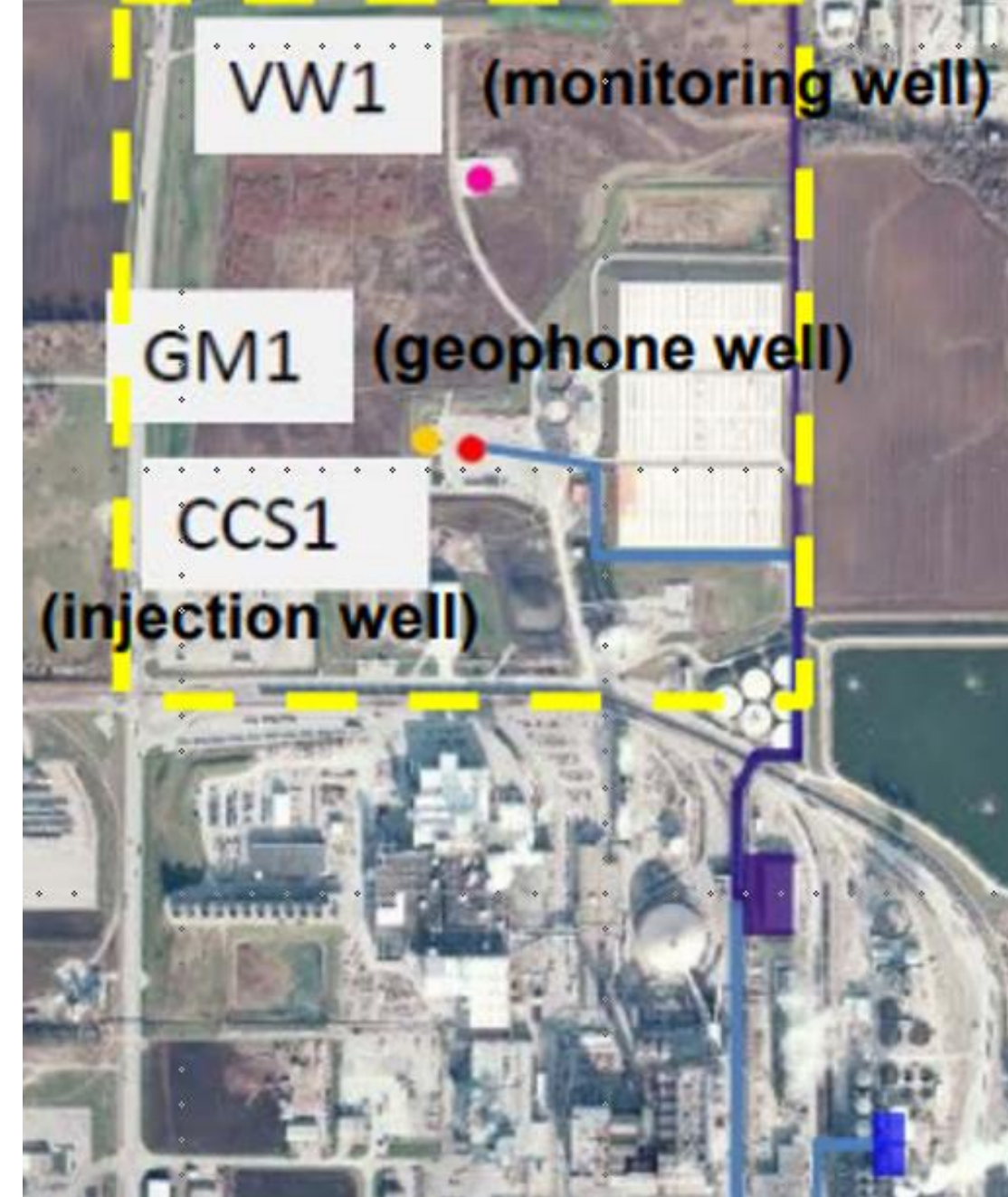


Figure 1. Map of the IBDP site with locations of the drilled wells.

METHODOLOGY

The approach implemented in this study is similar to that reported in the previous studies on microseismic-geomechanical correlations for Marcellus shale in West Virginia and Pennsylvania (Zorn et al., 2019, 2017). Microseismic attributes derived from the analysis of the microseismic catalog were correlated with geomechanical parameters derived from the CCS1 well logs of IBDP. The microseismic data were analyzed through the event cloud, crossing Mt. Simon and Argenta sandstones. The microseismic catalog was used to create pseudo-logs of moment magnitude (Mw), b-value, and event count. The vertical moving-average sampling of microseismic data was completed and interpolated to match the geophysical well logs collected at the CCS1 well. This technique creates robust, high-resolution microseismic logs that show subtle changes in microseismic properties and allow direct cross-plotting of microseismic versus geophysical logs. Five geomechanical properties were chosen to form the framework to correlate with the microseismic data: Young's modulus (YM), Poisson's ratio (PR), brittleness, lambda-rho (LR), and mu-rho (MR). Additionally, natural gamma ray log was included as a useful measure of organic content. These microseismic-geomechanical hyperdimensional plots provide insights into the response of these sandstone formations to CO₂ injection. In the hyperdimensional space, there is a meaningful link between microseismicity and the elastic properties of the host rock. The calculation of microseismic pseudo-logs at the injection site and application of the hyperdimensional plot framework to the microseismic-geomechanical analysis in saline aquifers will inform operators in planning and forecasting reservoir responses to CO₂ injection.

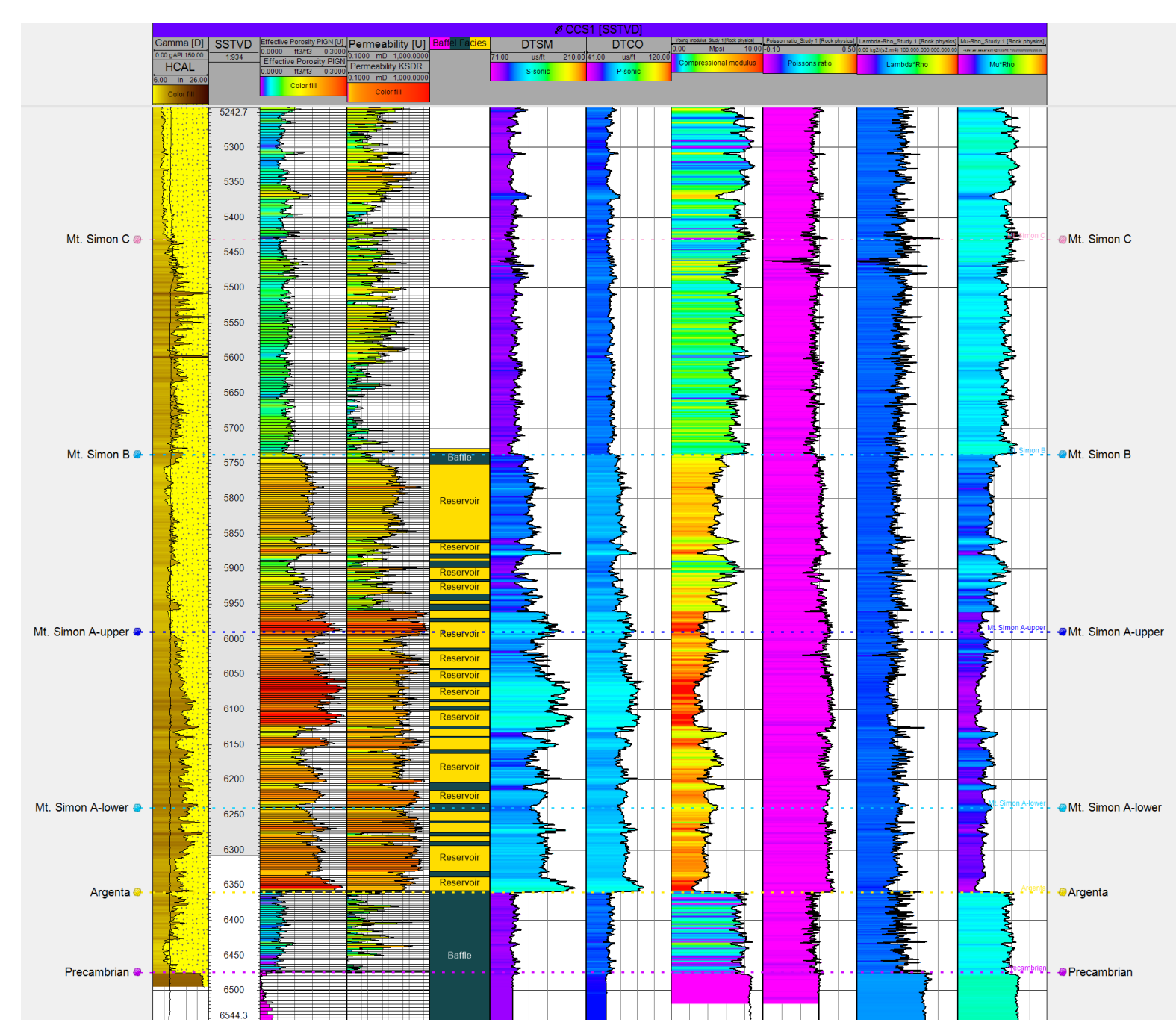


Figure 2. Composite well logs at CCS1 used in this study.

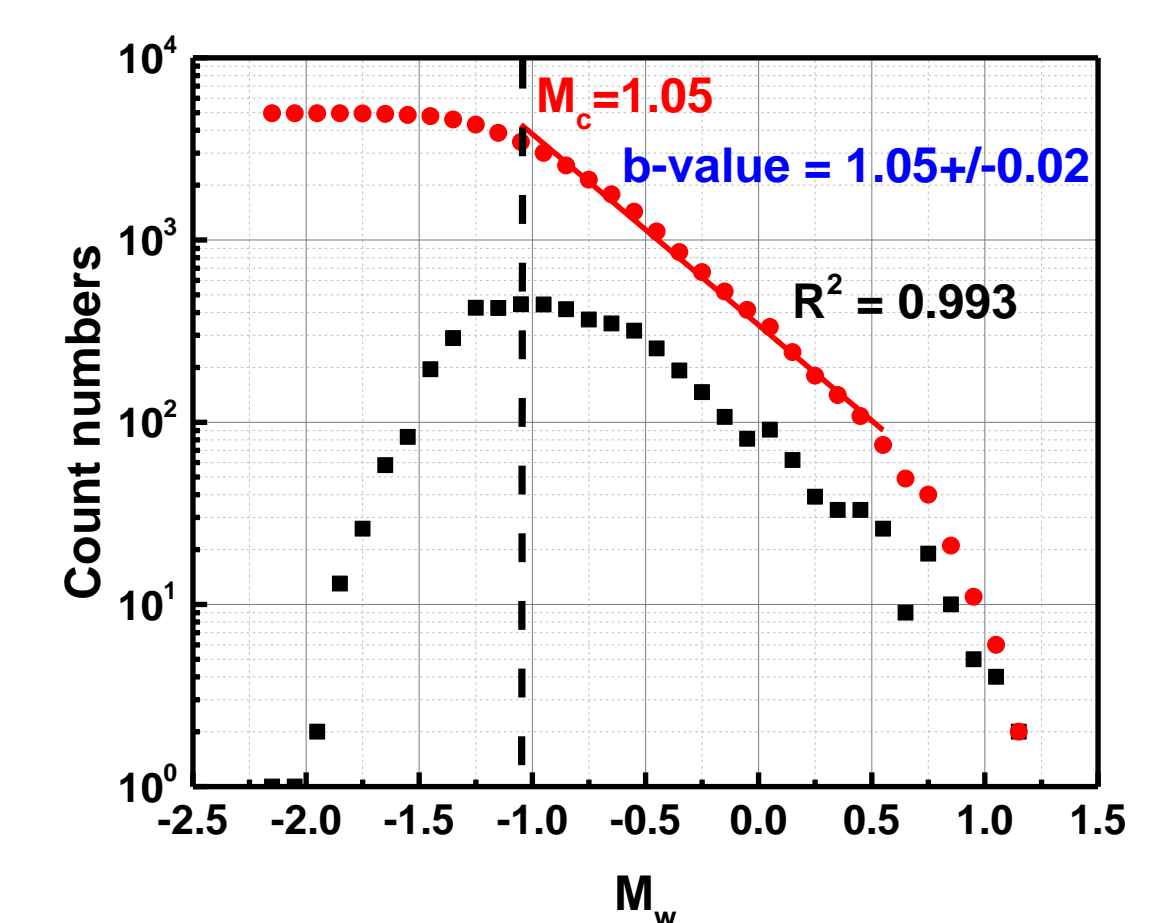


Figure 3. Mc and b-value for the entire IBDP catalog.

The magnitude of completeness (M_c) is the minimum magnitude above which the distribution still follows the Gutenberg-Richter power law relationship. The value of M_c is calculated by using the catalog for the entire magnitude range.

The seismogenic **b-value** is the slope of the linear portion of the log10 (frequency) versus magnitude distribution in a seismic catalog, and it is an indicator of in situ stress conditions.

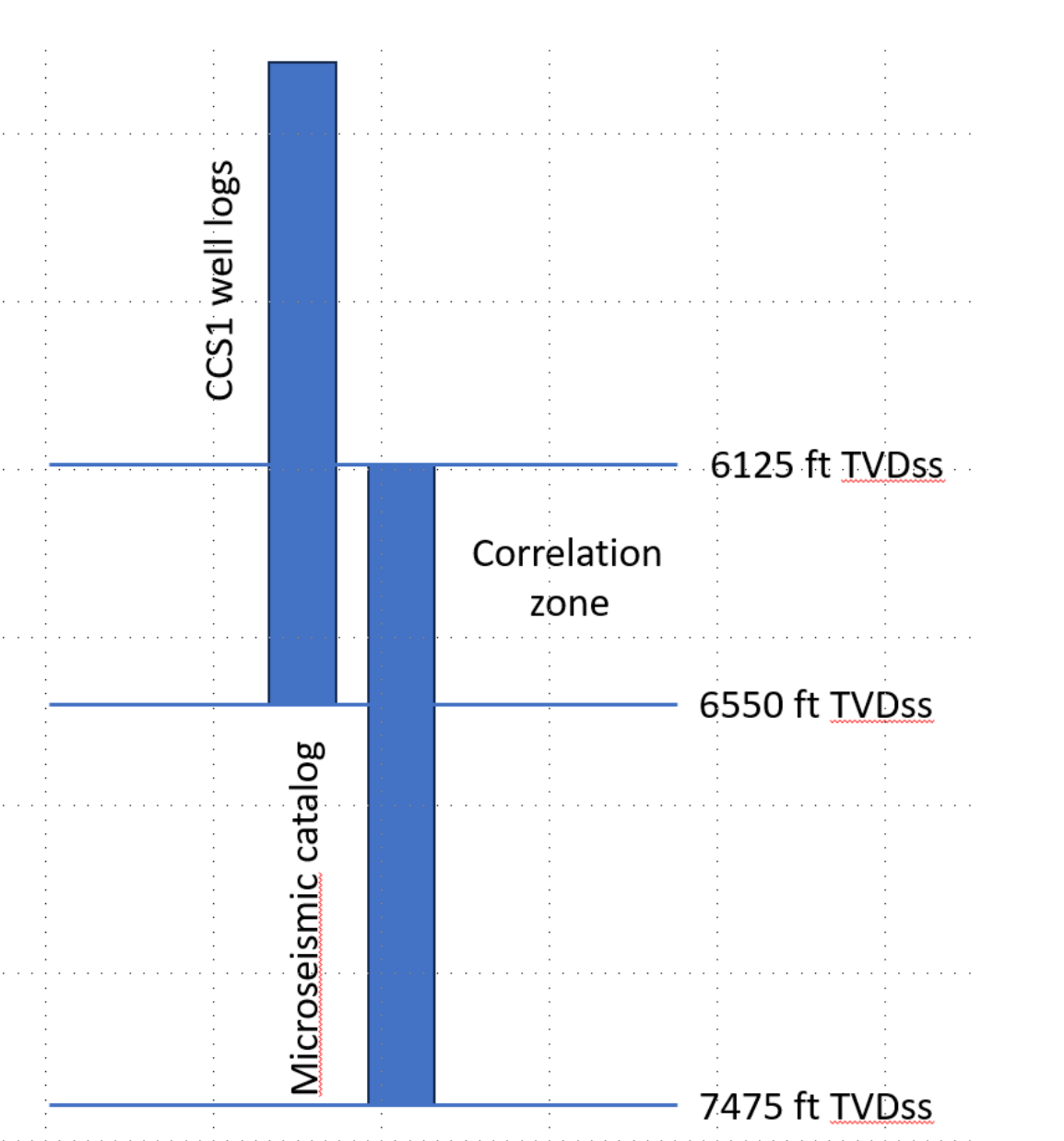


Figure 4. Correlation zone interval of overlapping well log data and microseismic catalog.

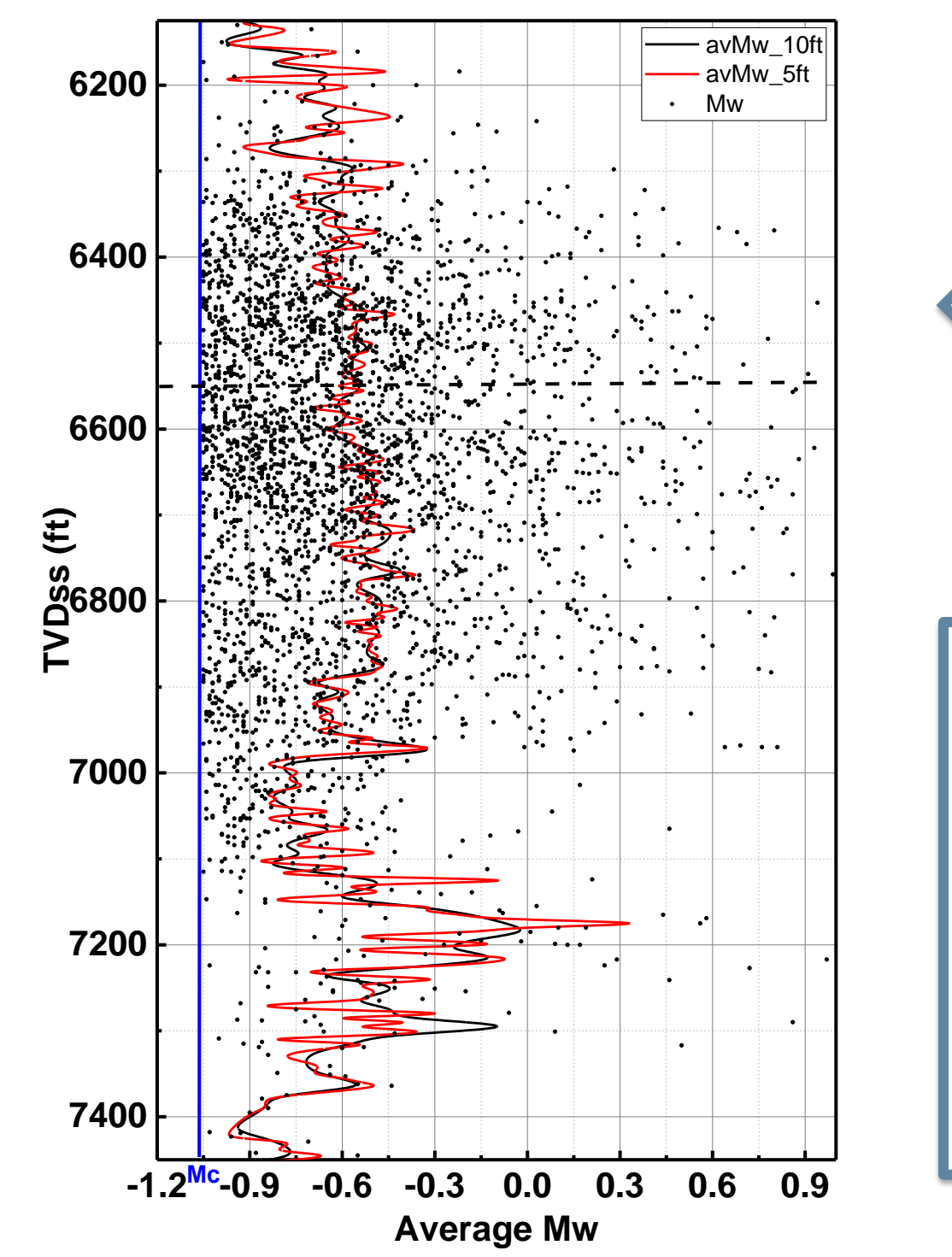


Figure 5. The Mw pseudo-logs (5- and 10-ft scales) superimposed on the microseismic cloud from which it was calculated. The black dashed line indicates a depth level of the igneous unconformity.

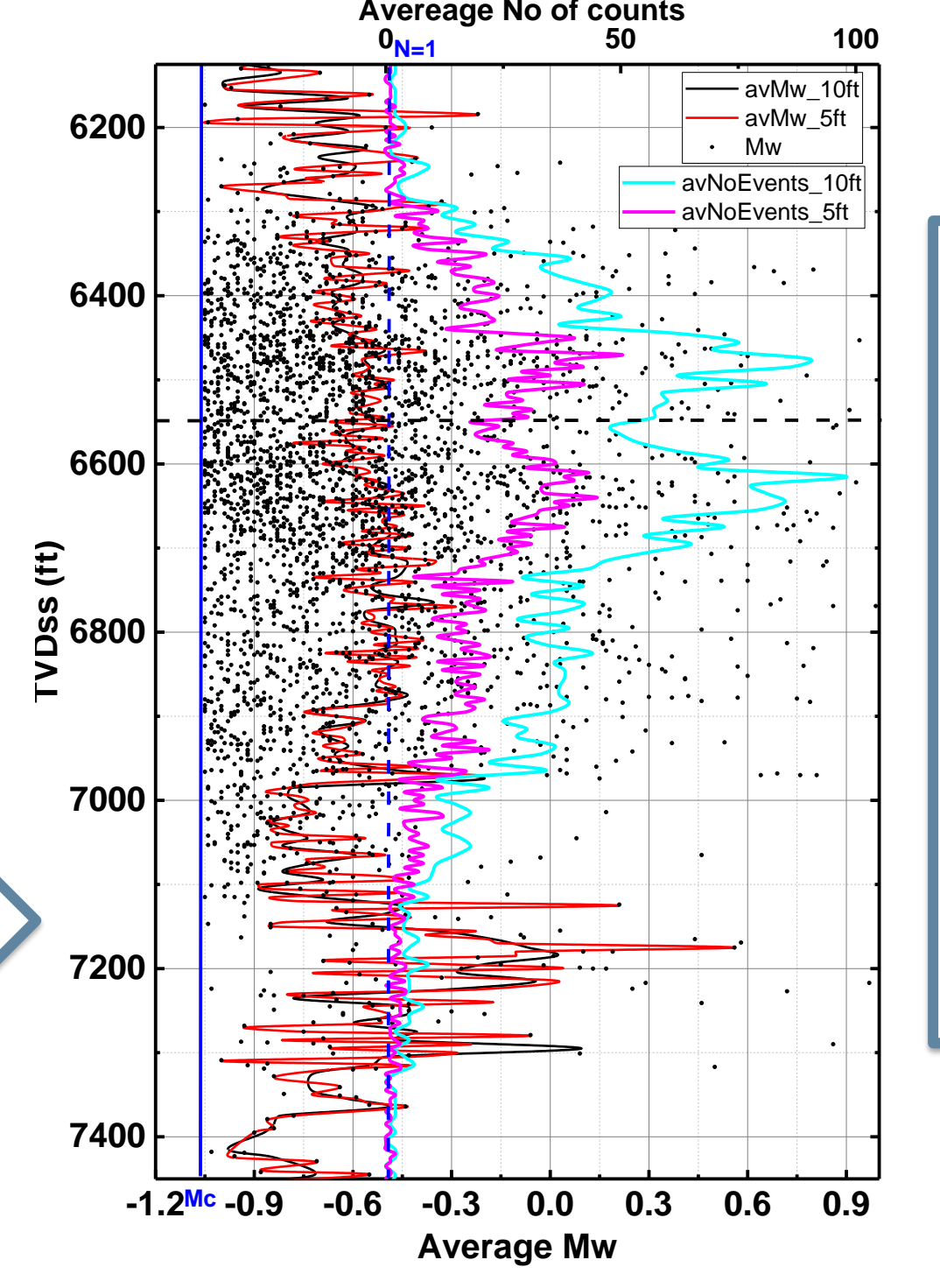


Figure 6. The Mw and event count pseudo-logs (5- and 10-ft scales) superimposed on the microseismic cloud from which they were calculated. The black dashed line indicates a depth level of the igneous unconformity.

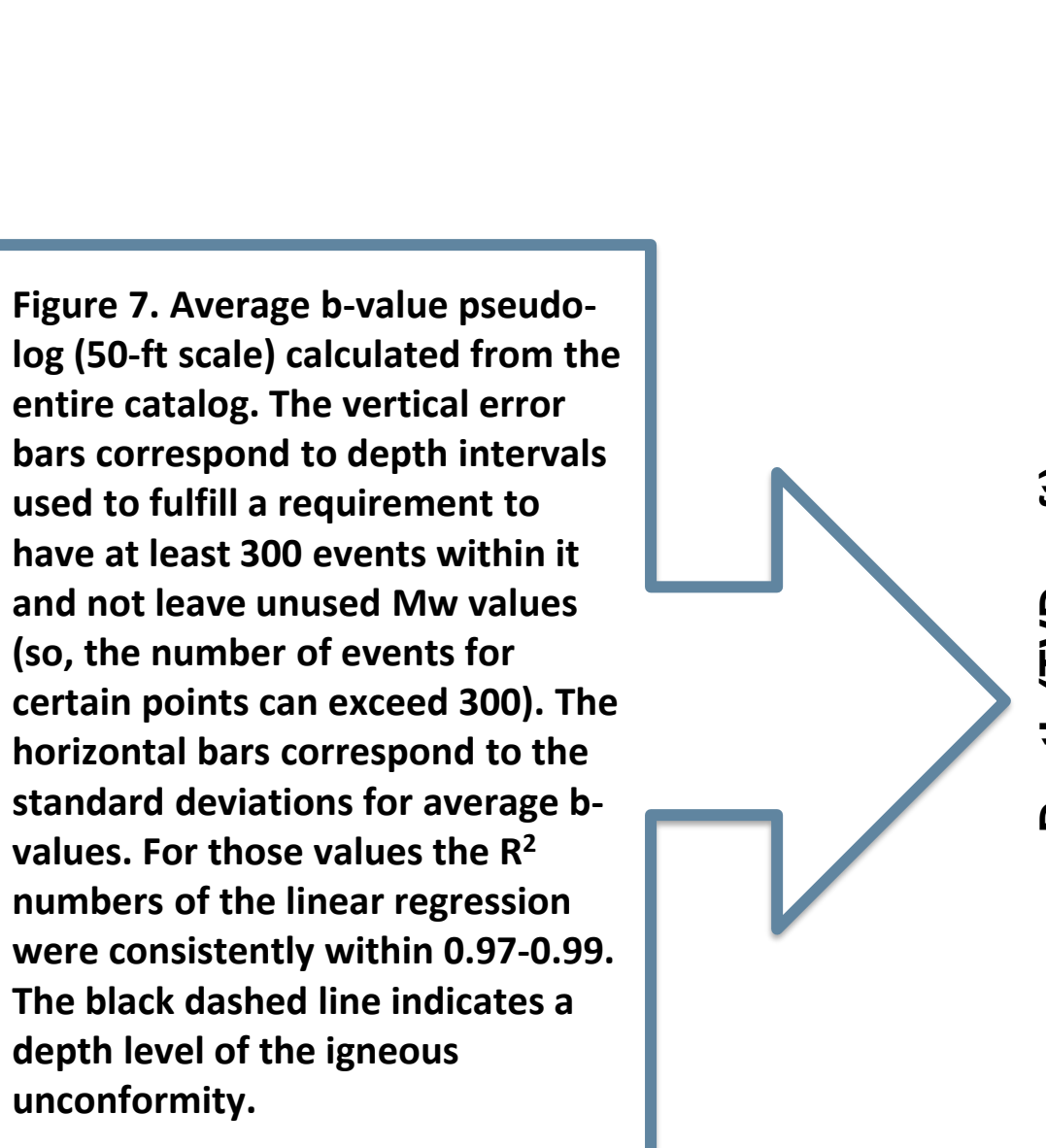


Figure 7. Average b-value pseudo-log (50-ft scale) calculated from the entire catalog. The vertical error bars correspond to depth intervals used to fulfill a requirement to have at least 300 events within it and not leave unused Mw values (so, the number of events for certain bars can exceed 300). The horizontal bars correspond to the standard deviations for average b-values. For those values the R² numbers of the linear regression were consistently within 0.97-0.99. The black dashed line indicates a depth level of the igneous unconformity.

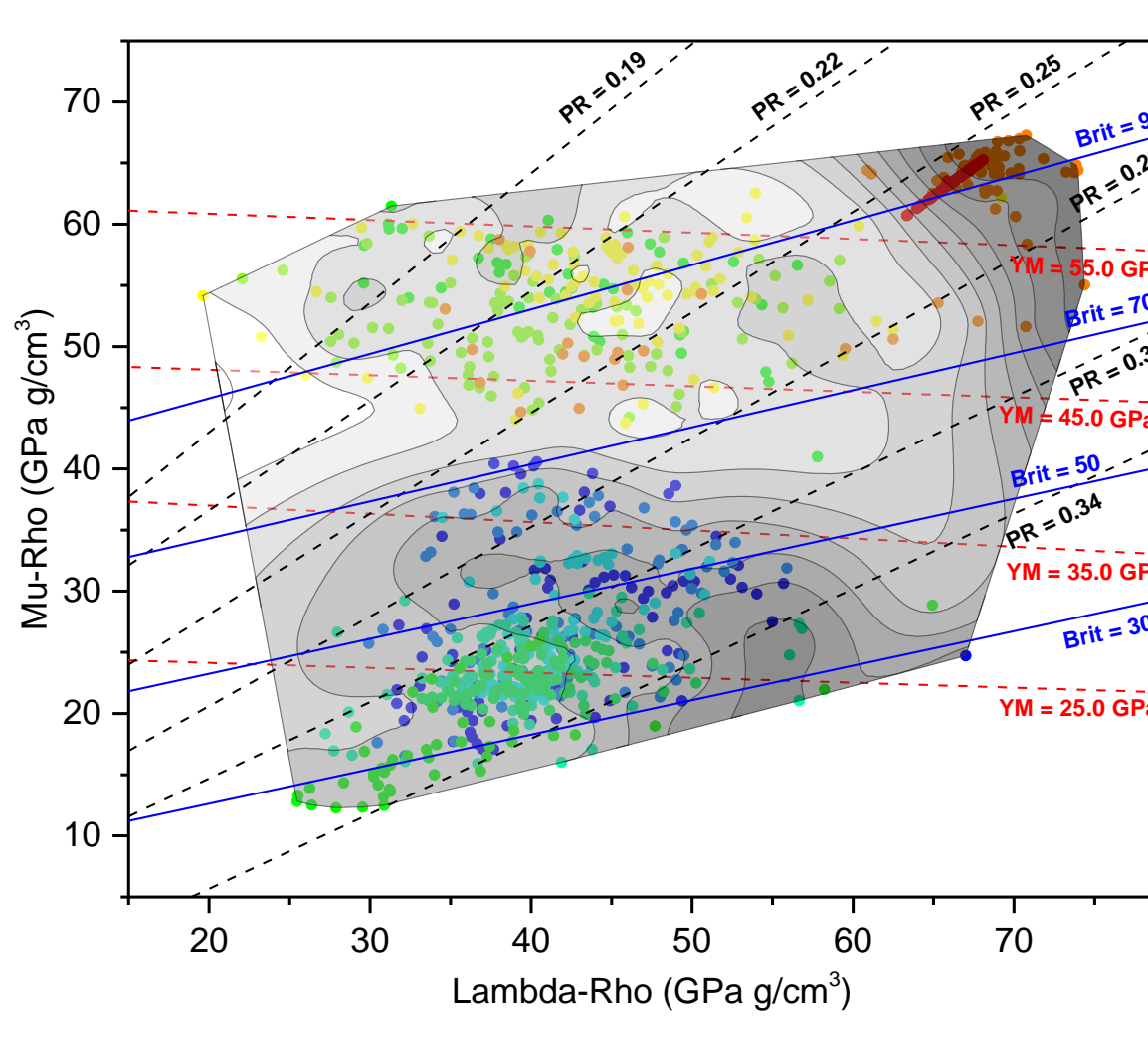
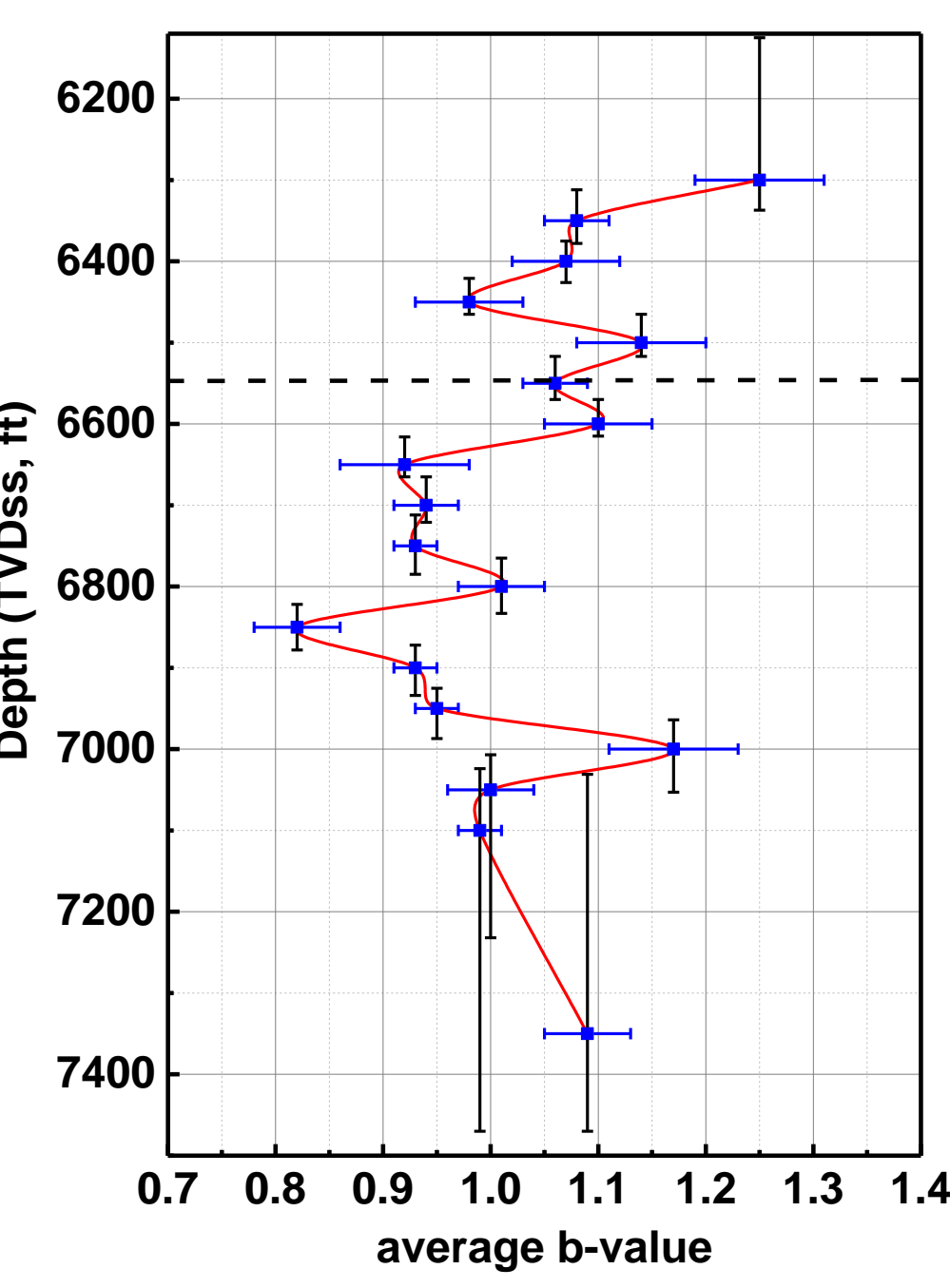


Figure 8. The hyperdimensional plot using depth as a colored attribute. The Argenta Formation (6,360-6,550 TVDss ft); the Lower/Upper Mt. Simon A sandstone is located within the 6,125-6,360 TVDss ft range.

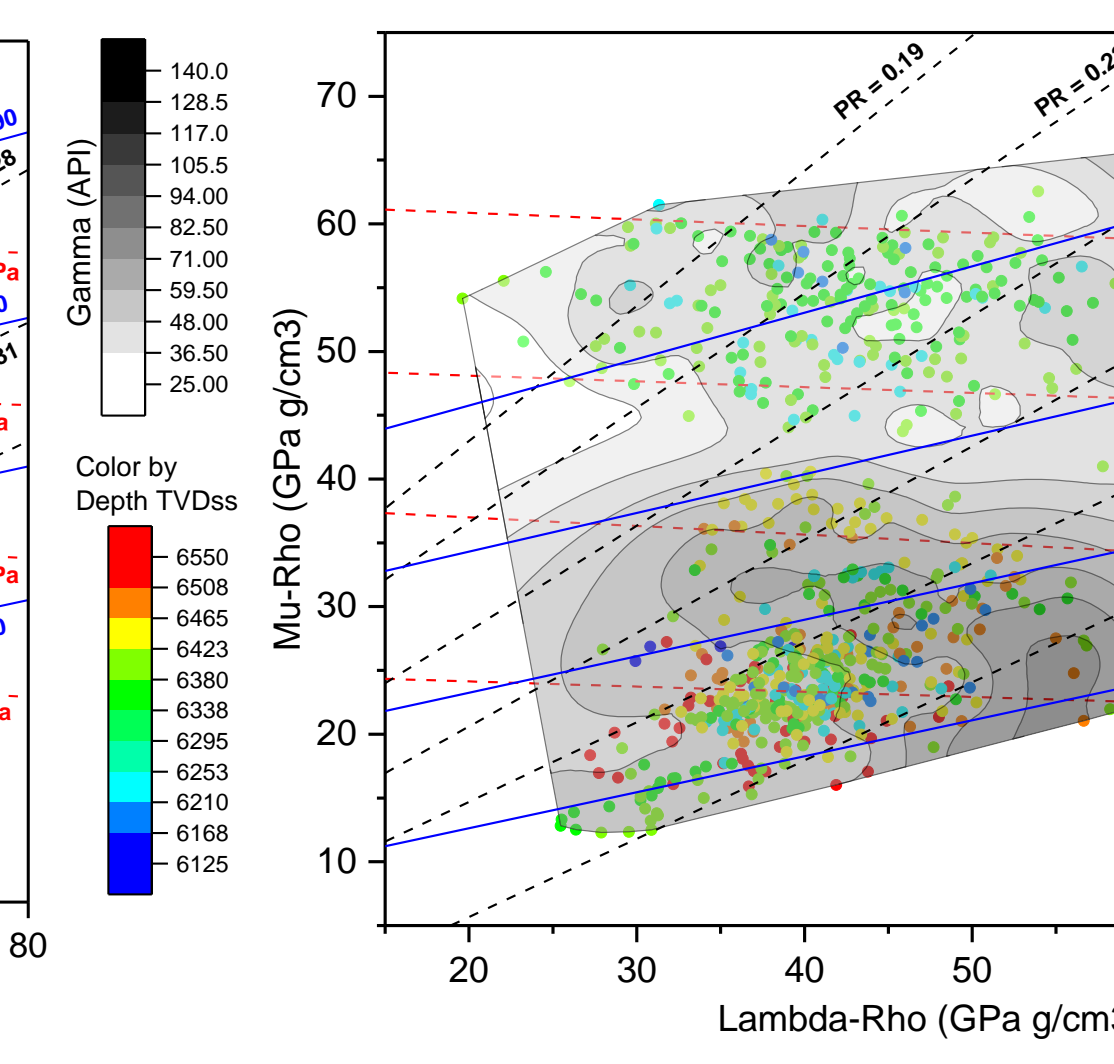


Figure 9. The hyperdimensional plot using the average moment magnitude of microseismicity as a colored attribute.

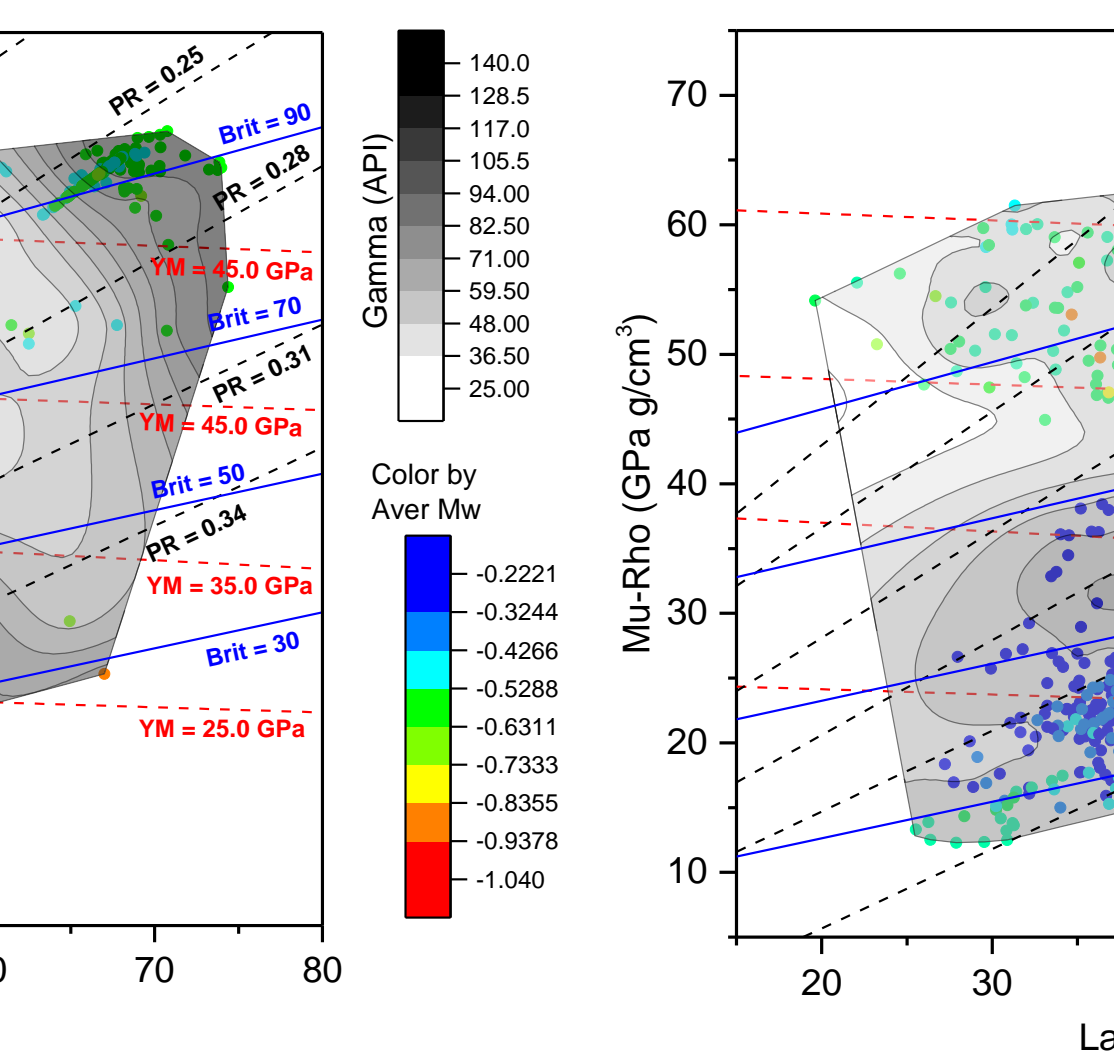


Figure 10. The hyperdimensional plot using the average microseismic event count as a colored attribute.

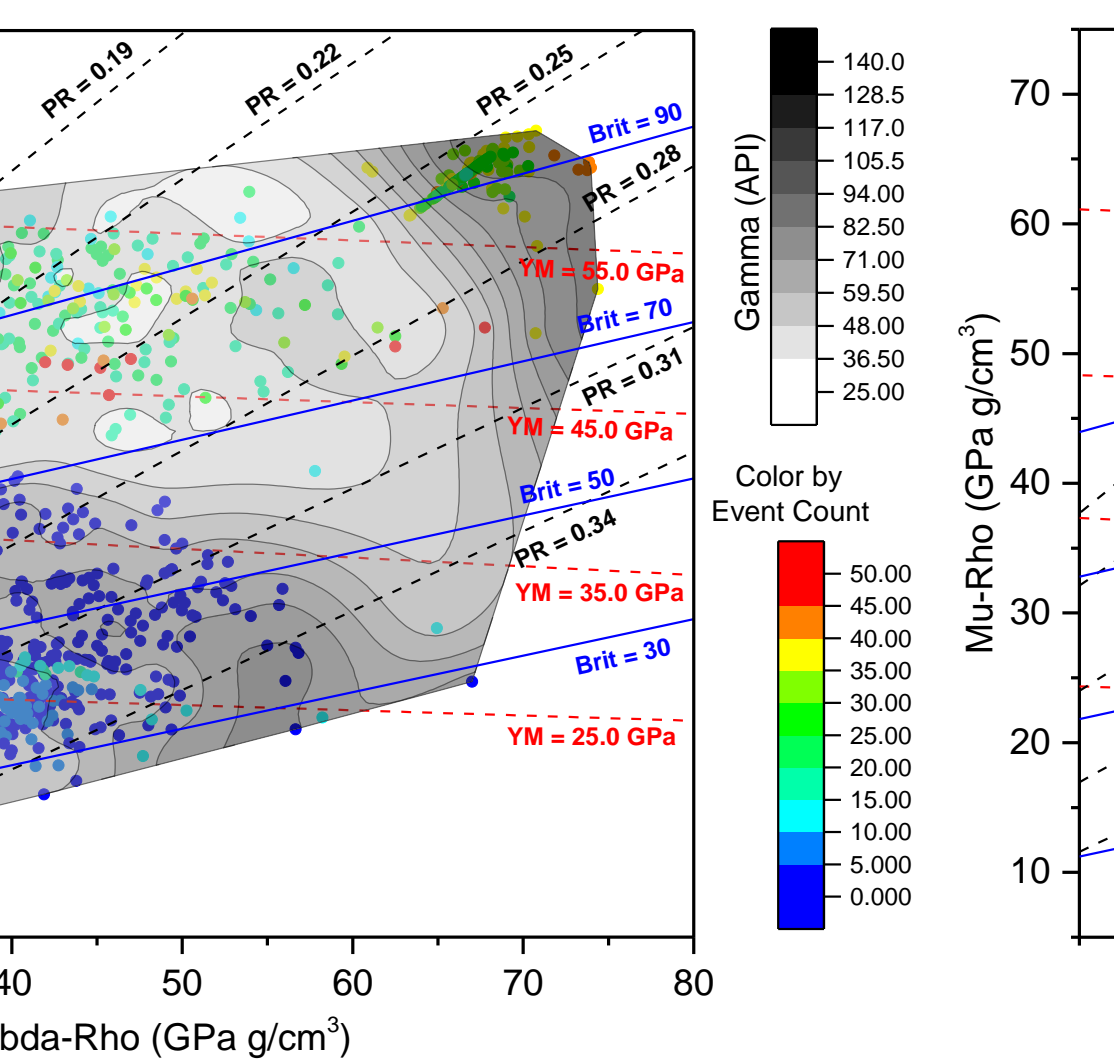


Figure 11. The hyperdimensional plot using the seismogenic b-value of microseismicity as a colored attribute.

$$MR = (V_s * Rho)^2 = SI^2$$

$$LR = (V_p * Rho)^2 - 2 * (V_s * Rho)^2 = AI^2 - 2 * SI^2$$

Rho – density, Vp and Vs, compressional and shear wave velocities

$$YM = \frac{\sigma}{\epsilon} \quad PR = \frac{d\epsilon_{trans}}{d\epsilon_{axial}}$$

σ – stress, ϵ – strain; $d\epsilon_{trans}$ and $d\epsilon_{axial}$ transverse and axial strains

$$BRIT_{YM} = \left(\frac{YM - 1}{8 - 1}\right) * 100 \quad BRIT_{PR} = \left(\frac{PR - 0.4}{0.15 - 0.4}\right) * 100$$

$$BRIT_{TOTAL} = \frac{(BRIT_{YM} + BRIT_{PR})}{2}$$

YM – Young Modulus, PR – Poisson's ratio

Conclusions

- Increasing/decreasing YM results in increasing/decreasing the event magnitude.
- YM is a measure of material stiffness connected to resistance to rock deformation under stress.
- The lowest number of events occur in the region of highest PR and low YM, and microseismicity is most abundant where PR is lowest. PR is a measure of material toughness related to the resistance to fracturing when stressed.
- High/low b-value occurred in mid to low/high YM and high/low gamma (organic content) region. Since low YM implies low material stiffness, low YM and high organic content allow the internal stress to be readily redistributed, avoiding high stress conditions, and resulting in a higher b-value.

Acknowledgement

This work was performed in support of the U.S. Department of Energy's (DOE) SMART Research Initiative. We would like to thank Illinois State Geologic Survey for providing microseismic data and pumping data from the IBDP site that was used in this fracture network mapping study.

References

- Liu, G., Siriwardane, H., Kumar, A., Harbert, W., Crandall, D., and Cunha, L., 2024. Fracture Analysis and Mapping in the Illinois Basin Carbon Dioxide Storage Site, American Rock Mechanics Association Conference, Golden, Colorado.
- Zorn, E., Kumar, A., Harbert, W., Hammack, R. 2019. Geomechanical analysis of microseismicity in an organic shale: A West Virginia Marcellus Shale example. *Interpretation*, 7 (1), T231-T239.
- Zorn, E., W. Harbert, R. Hammack, et al. 2017. Geomechanical lithology-based analysis of microseismicity in organic shale sequences: a Pennsylvania Marcellus Shale example: *The Leading Edge*, 36, no.10, 845-851.

Disclaimer

This project was funded by the United States Department of Energy, National Energy Technology Laboratory, in part, through a site support contract. Neither the United States Government nor any agency thereof, nor any of their employees, nor the support contractor, nor any of their employees, makes any warranty, expressed or implied, or assumes any legal liability or responsibility for the accuracy, completeness, or usefulness of any information, apparatus, product, or process disclosed, or represents that its use would not infringe privately owned rights. Reference herein to any specific commercial product, process, or service by trade name, trademark, manufacturer, or otherwise, does not necessarily constitute or imply its endorsement, recommendation, or favoring by the United States Government or any agency thereof. The views and opinions of authors expressed herein do not necessarily state or reflect those of the United States Government or any agency thereof.

